Electronic Supplementary Material (ESI) for Dalton Transactions.

Cycloruthenated complexes: pH-dependent reversible cyclometallation and reactions with nitrite at octahedral ruthenium centers

Xianlong Su [a], Rongqing Zeng [b], Xianghong Li [a,*], Weijie Dang [a], Kaiyue Yao [a], Dingguo Tang [b,*]

[a] Key Laboratory of Catalysis and Materials Science of the State Ethnic Affairs Commission & Ministry of Education, South-Central University for Nationalities, Wuhan 430074, China

[b] College of Chemistry and Materials Science, South-Central University for Nationalities, Wuhan 430074, China

*Corresponding author, Email: lixhchem@mail.scuec.edu.cn; tdgpku@mail.scuec.edu.cn

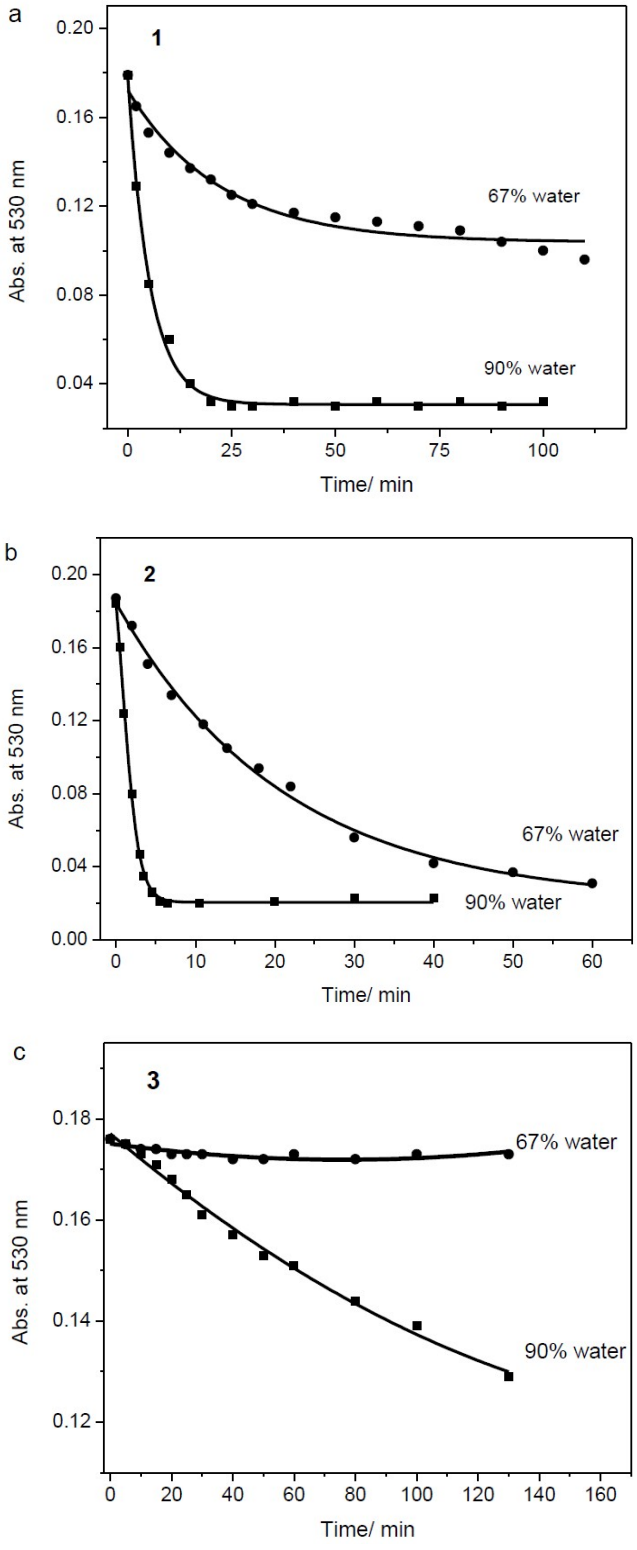

Figure S1 Time dependence of the absorption intensities of **1**(a), **2**(b), and **3**(c) at 530 nm in 90% v/v and 67% v/v water-ethanol solutions buffered at pH 2.47, respectively. The concentration of these complexes solutions was about 20 μM.

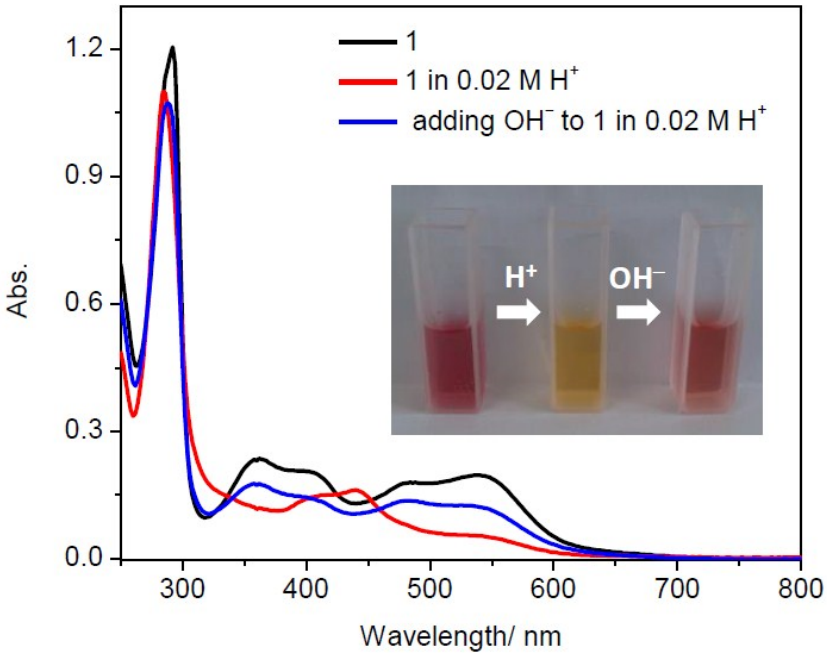

Figure S2 The absorption spectra of **1** (20 μM) under different conditions. Inset: The photograph of **1** in CH_3CN/ethanol/H_2O (v/v/v = 2:8:90), **1** in solution after titration of H^+, and subsequent treatment with OH^-, respectively**.**

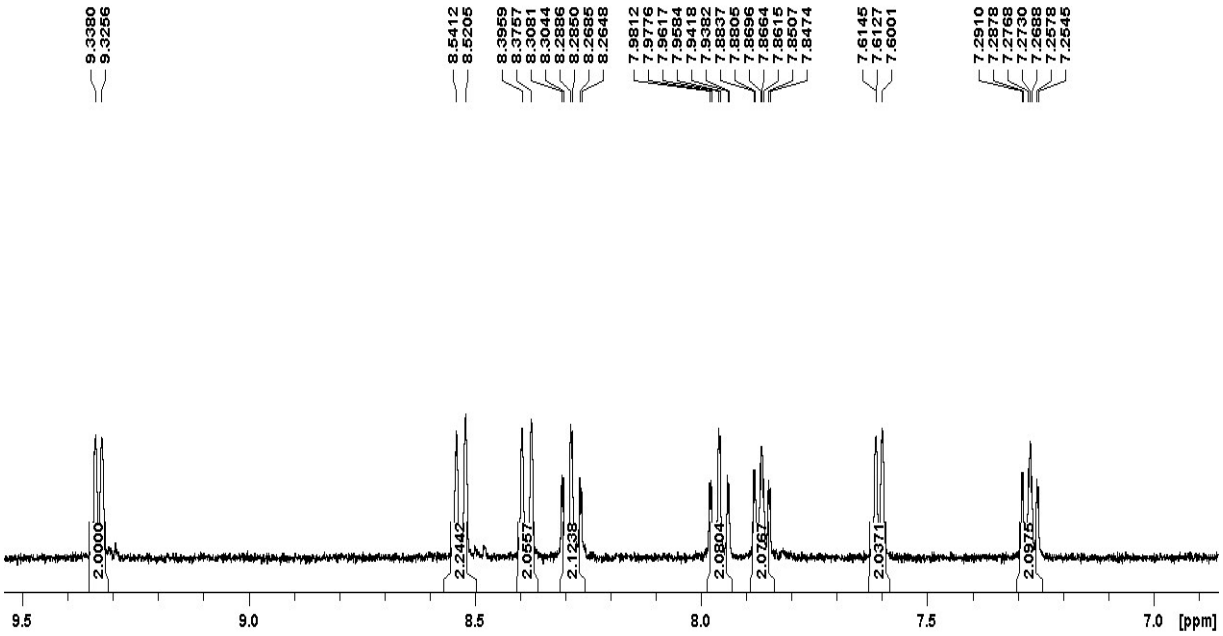

Figure S3 The ^{1}HNMR spectrum of $[Ru(bpy)_2(H_2O)Cl]PF_6$ (**5**) in CD_3CN

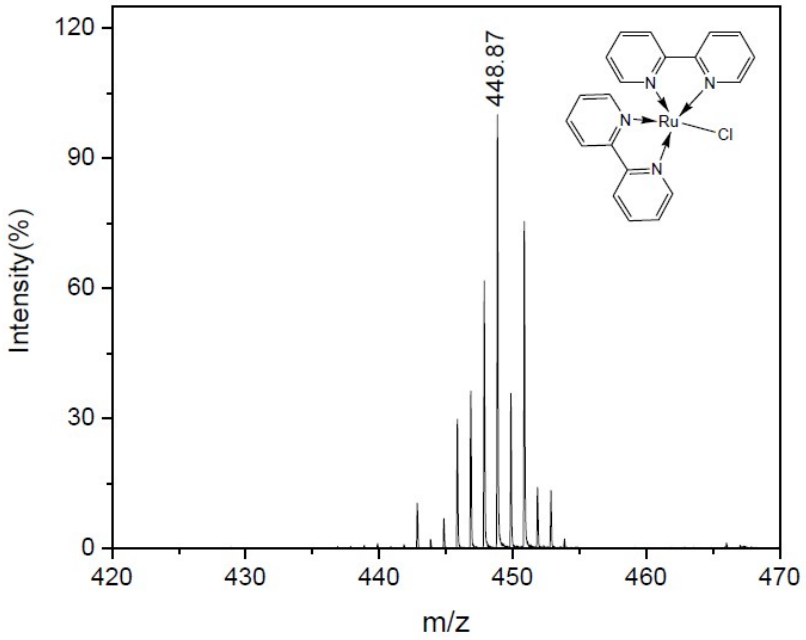

Figure S4 The MS spectrum of $[Ru(bpy)_2(H_2O)Cl]PF_6$ (**5**)

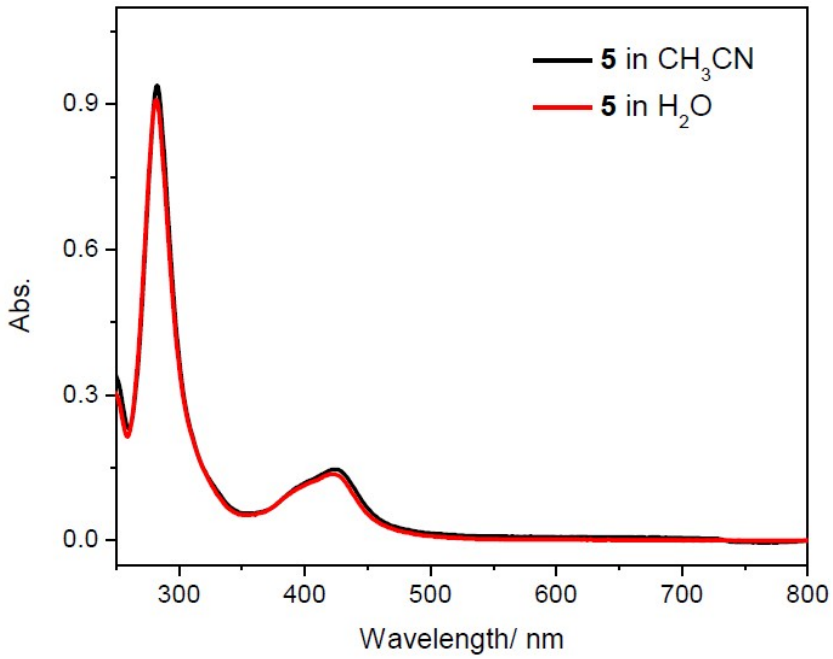

Figure S5 The absorption spectra of $[Ru(bpy)_2(H_2O)Cl]PF_6$ (**5**)

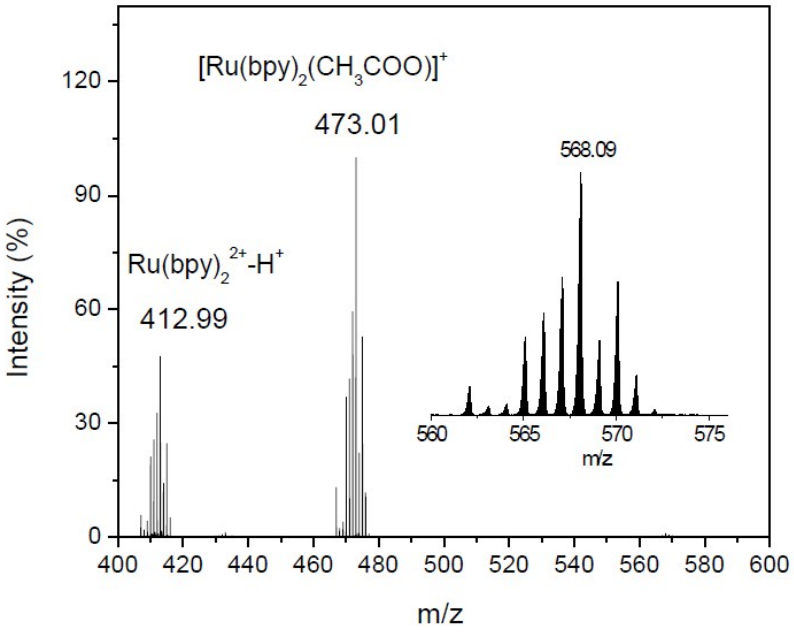

Figure S6 The MS spectrum of the Ru(ppy)$(bpy)_2^+$ in HAc solution. Insert: The MS spectrum of the Ru(ppy)$(bpy)_2^+$ (1).

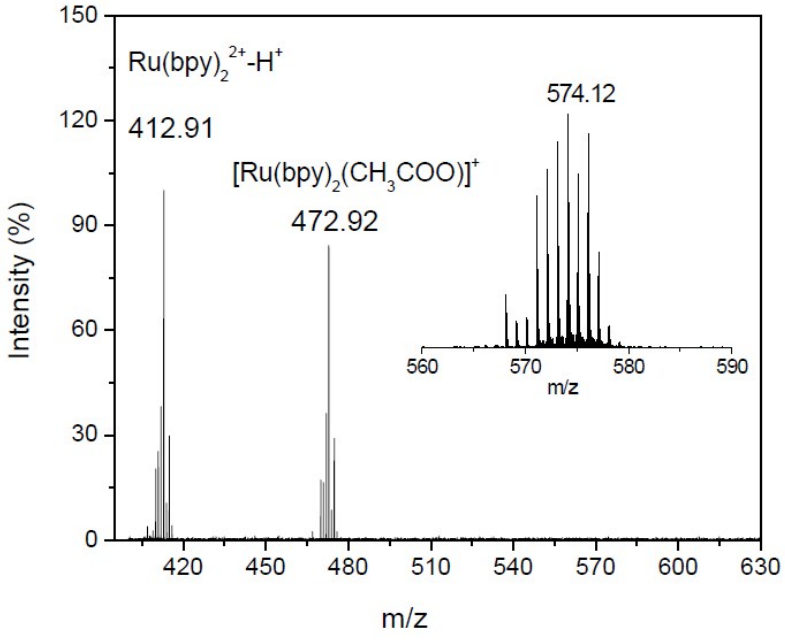

Figure S7 The MS spectrum of the Ru(thpy)$(bpy)_2^+$ (**2**) in HAc solution. Insert: The MS spectrum of the Ru(thpy)$(bpy)_2^+$ (**2**).

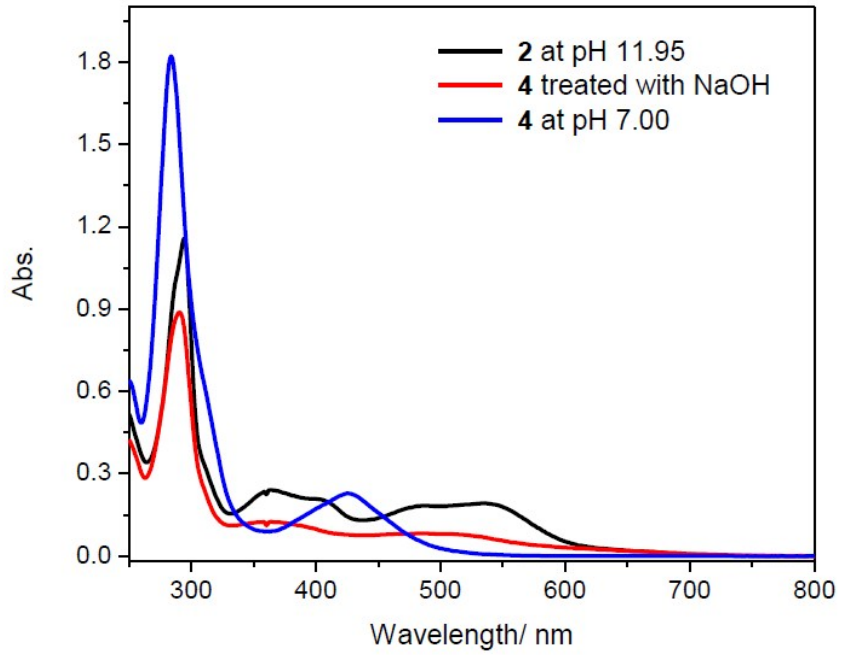

Figure S8 The absorption spectra of **2** (20 μM) and **4** (20 μM) under different conditions, respectively.

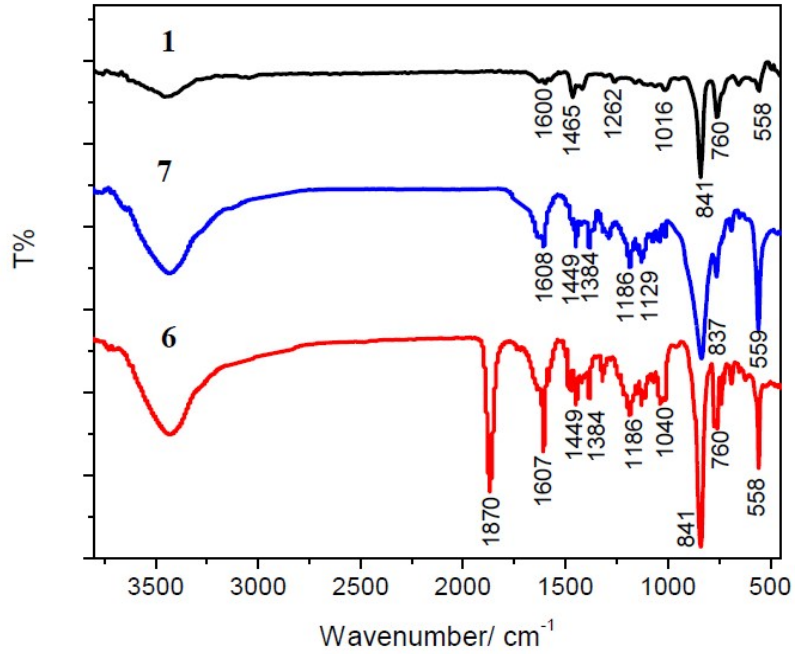

Figure S9 The IR spectra of $[Ru(ppy)(bpy)_2]PF_6$ (1), $[Ru(ppy)(bpy)(NO)Cl]PF_6$ (**6**) , and $[Ru(ppyNO)(bpy)_2](PF_6)_2$ (**7**), respectively.

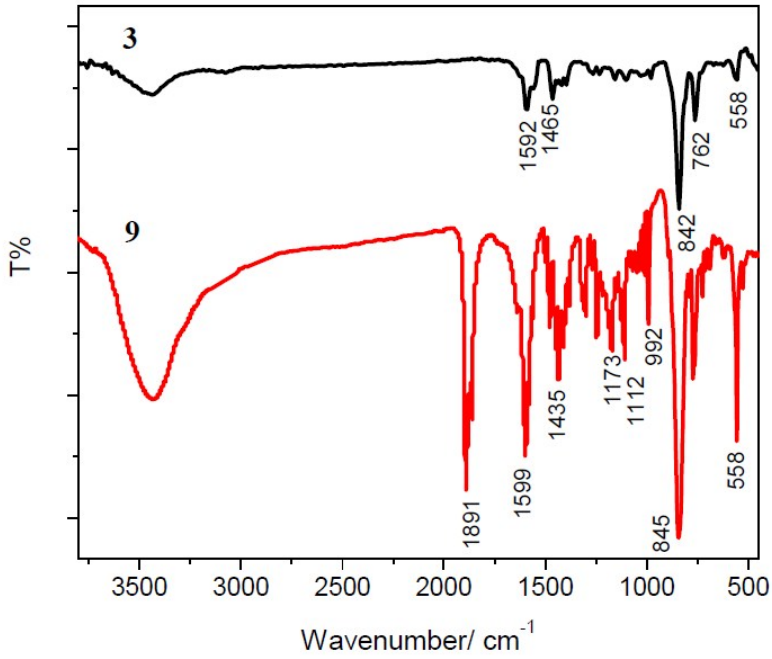

Figure S10 The IR spectra of $[Ru(dfppy)(bpy)_2]PF_6$ (**3**) and $[Ru(dfppy)(bpy)(NO)Cl]PF_6$ (**9**), respectively.

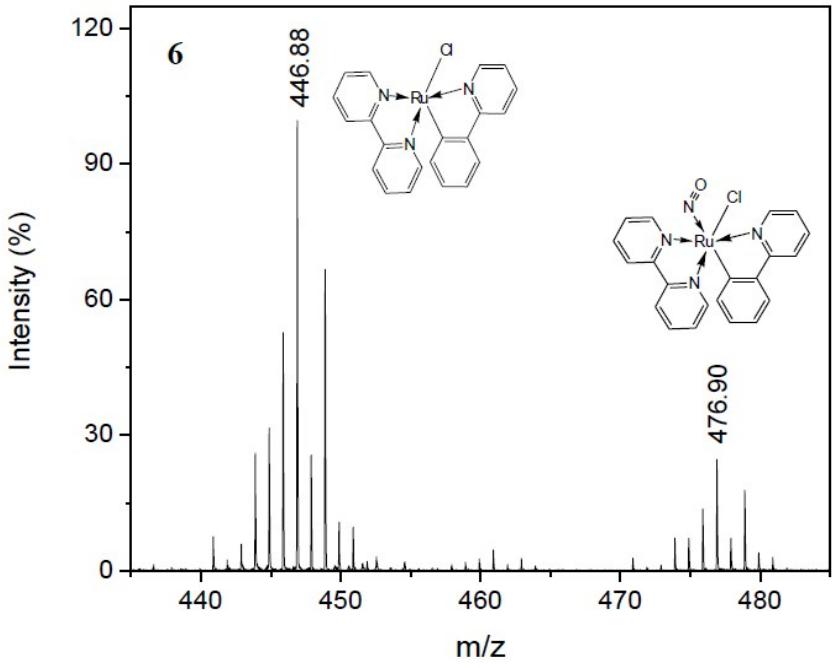

Figure S11 The MS spectrum of $[Ru(ppy)(bpy)(NO)Cl]PF_6$ (**6**).

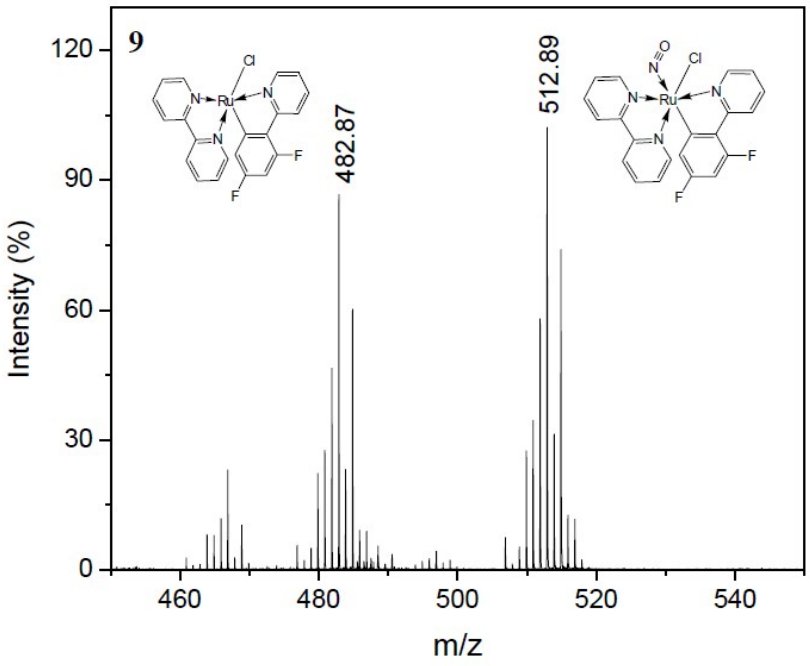

Figure S12 The MS spectrum of [Ru(dfppy)(bpy)(NO)Cl]PF_6 (**9**).

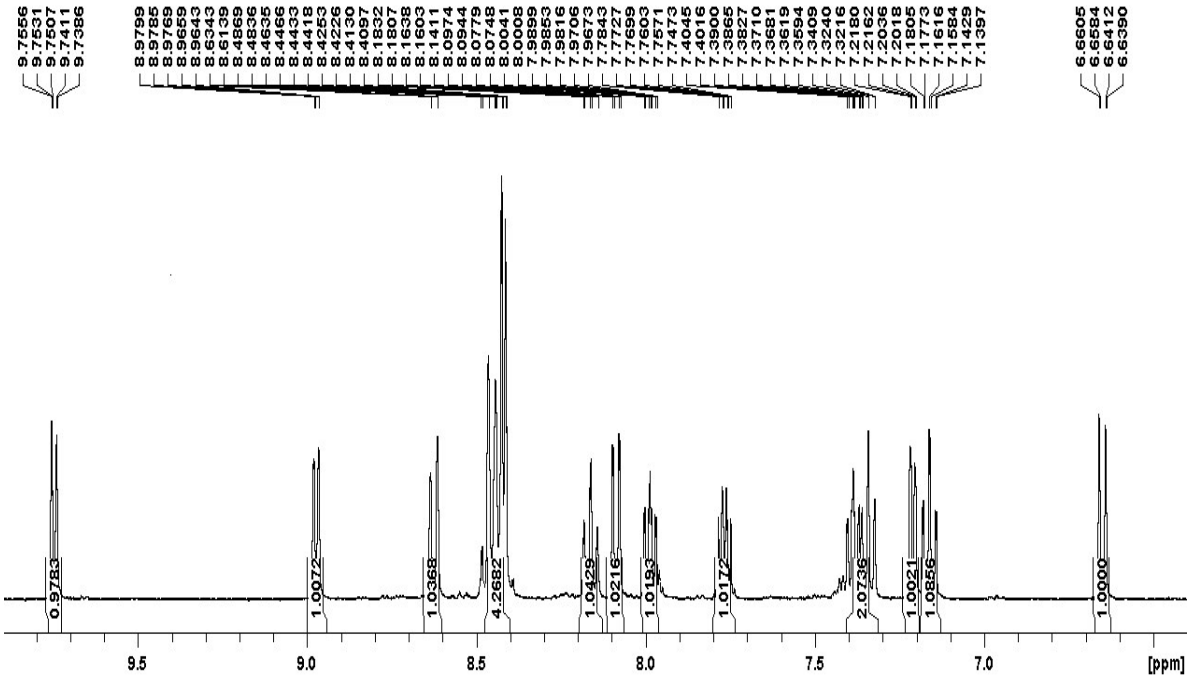

Figure S13 The ^{1}HNMR spectrum of [Ru(ppy)(bpy)(NO)Cl]PF_6 (**6**) in CD_3CN.

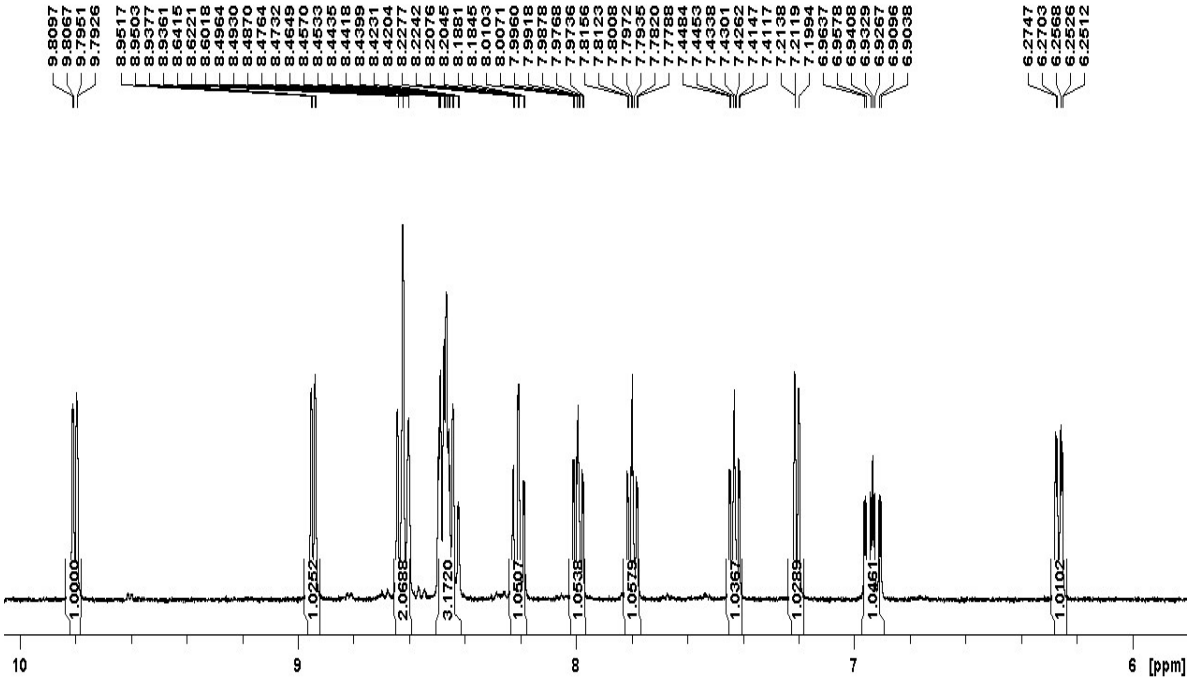

Figure S14 The ^{1}HNMR spectrum of [Ru(dfppy)(bpy)(NO)Cl]PF_6 (**9**) in CD_3CN.

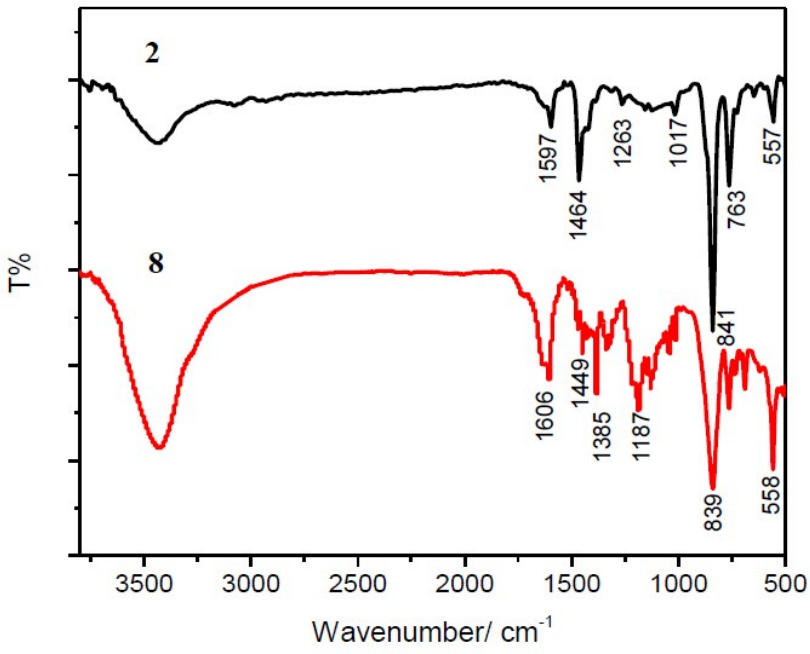

Figure S15 The IR spectra of [Ru(thpy)$(bpy)_2$]PF_6 (**2**) and [Ru(thpyNO)$(bpy)_2$]$(PF_6)_2$ (**8**), respectively.

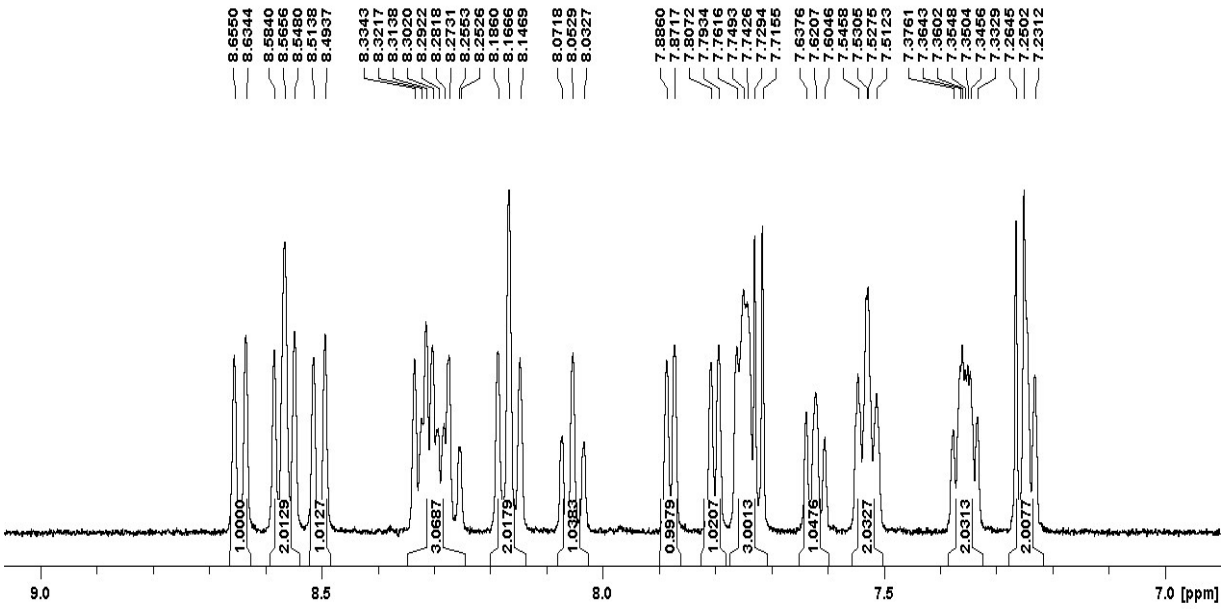

Figure S16 The ^{1}HNMR spectrum of [Ru(thpyNO)(bpy)$_2$](PF$_6$)$_2$ (**8**) in CD_3CN.

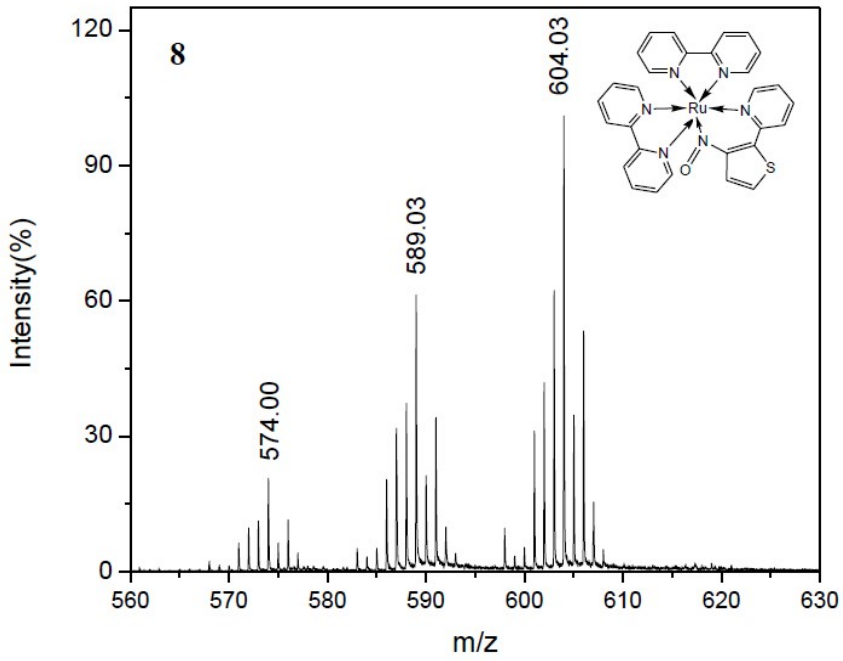

Figure S17 The MS spectrum of [Ru(thpyNO)(bpy)$_2$](PF$_6$)$_2$ (**8**).

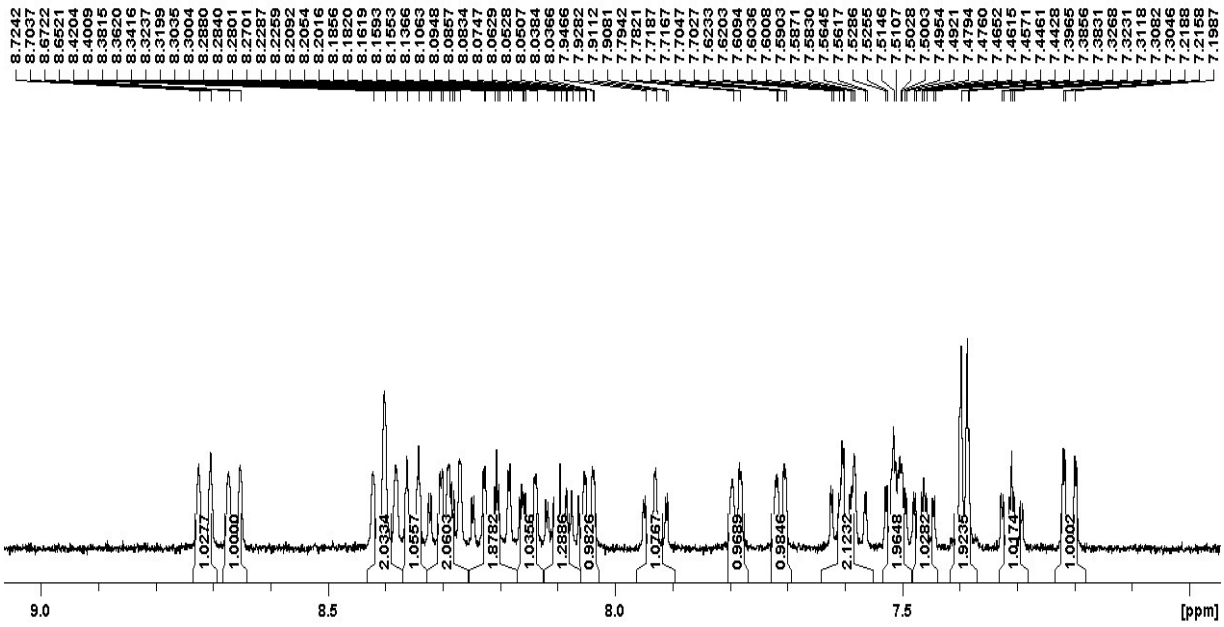

Figure S18 The ^{1}HNMR spectrum of $[Ru(ppyNO)(bpy)_2](PF_6)_2$ (**7**) in CD_3CN.

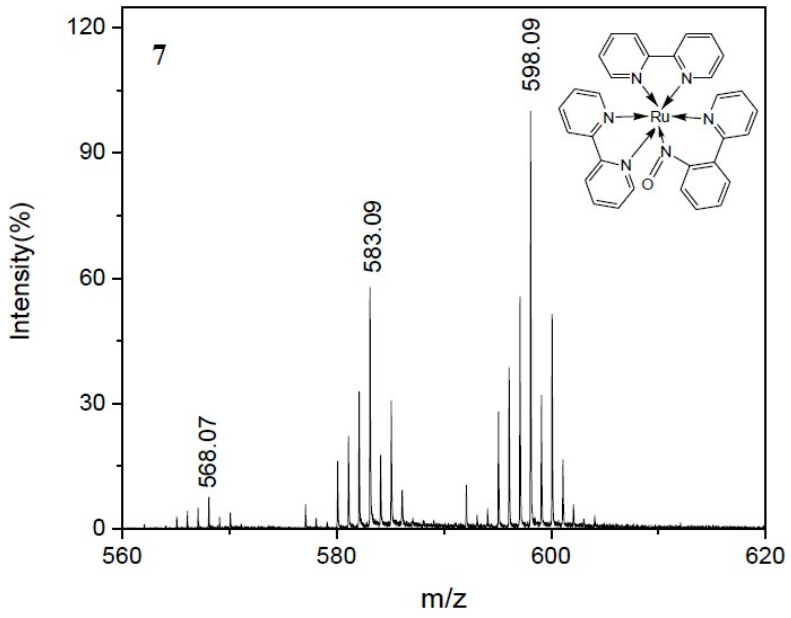

Figure S19 The MS spectrum of $[Ru(ppyNO)(bpy)_2](PF_6)_2$ (**7**).

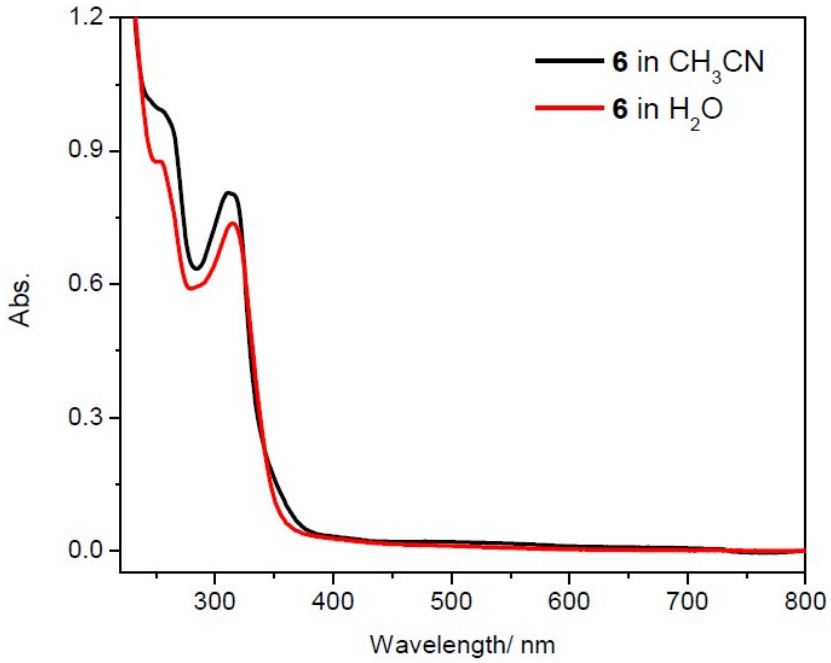

Figure S20 The absorption spectra of [Ru(ppy)(bpy)(NO)Cl]PF_6 (**6**).

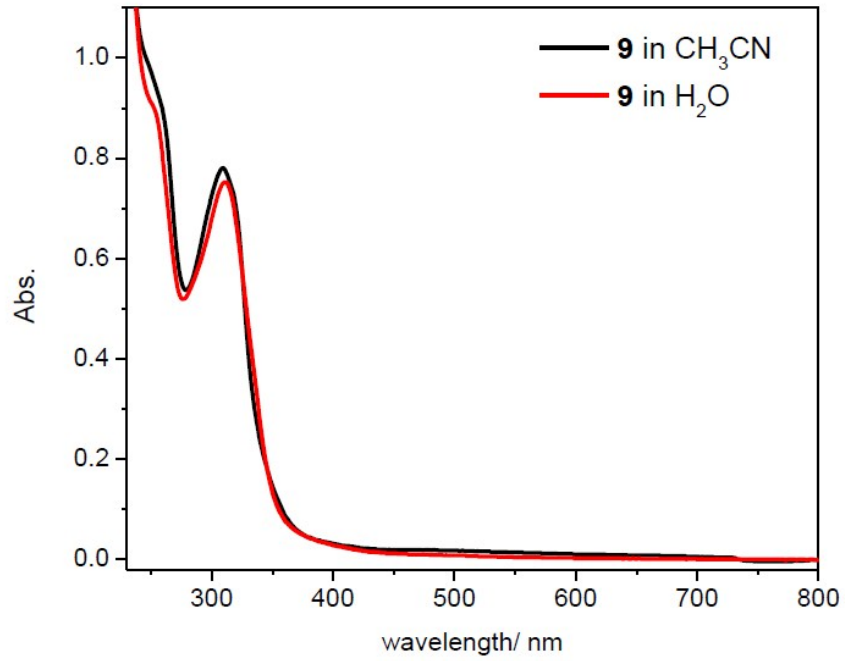

Figure S21 The absorption spectra of [Ru(dfppy)(bpy)(NO)Cl]PF_6 (**9**).

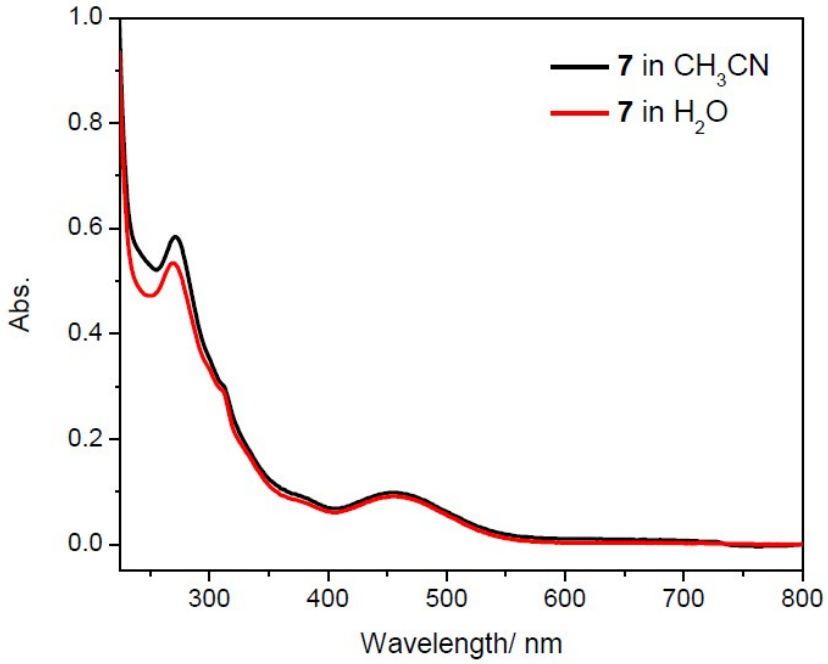

Figure S22 The absorption spectra of $[Ru(ppyNO)(bpy)_2](PF_6)_2$ (**7**).

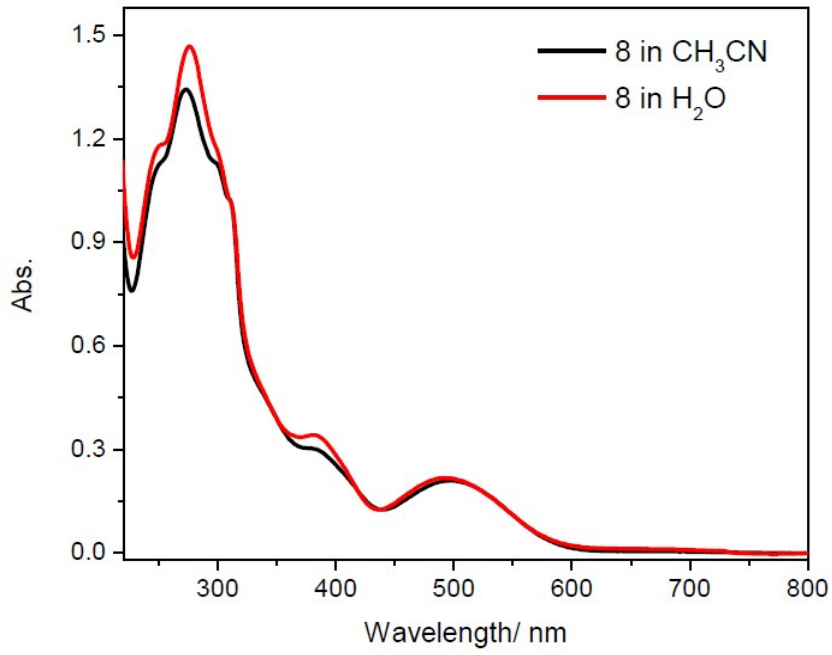

Figure S23 The absorption spectra of $[Ru(thpyNO)(bpy)_2](PF_6)_2$ (**8**).

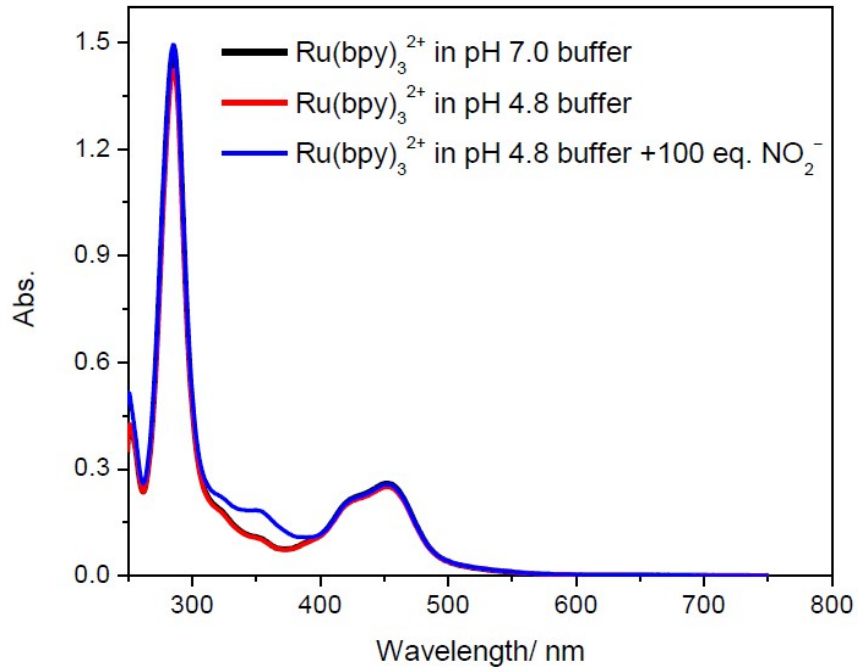

Figure S24 The absorption spectra of $Ru(bpy)_3^{2+}$ (20 μM) in CH_3CN/ethanol/ Briton-Robinson buffer solutions (v/v/v=2:8:90).

Table 1. Crystal data and structure refinement for **6**.

Empirical formula	$C_{42}\ H_{32}\ Cl_2\ F_{12}\ N_8\ O_2\ P_2\ Ru_2(CH_2Cl_2)$	
Formula weight	1328.66	
Temperature	173(2)K	
Wavelength	0.71073 Å	
Crystal system	Monoclinic	
Space group	P2(1)/c	
Unit cell dimensions	a = 12.2899(5) Å	α= 90.00°
	b = 16.2558(6) Å	β= 114.6440(10)°
	c = 13.4995(5) Å	γ =90.00°
Volume ($Å^3$)	2451.31(16)	
Z, Density (mg/m^3, calculated)	2, 1.800	
Absorption coefficient (mm^{-1})	0.993	
F(000)	1316	
Theta range for data collection(°)	3.01 to 28.35	
Index ranges	-16<=h<=15, -21<=k<=21, -17<=l<=18	
Reflections collected	23055	
Independent reflections [$R_{(int)}$]	6098 [0.0372]	
Completeness to theta = 28.35°	99.6 %	
Refinement method	Full-matrix least-squares on F^2	
Data / restraints / parameters,	6098 / 0 / 343	
Goodness-of-fit on F^2	1.015	
Final R indices [I>2σ(I)]	R_1 =0.0332, wR_2 = 0.0709	
R indices (all data)	R_1 = 0.0472, wR_2 = 0.0767	
Largest diff. peak and hole (e $Å^{-3}$)	0.807 And -0.850	

Table 2. Selected bond lengths [Å] and angles [°] for **6**.

Ru(1)−N(1)	2.105(2)	Ru(1)−N(2)	2.0661(19)	Ru(1)−N(3)	2.075(2)
Ru(1)−N(4)	1.740(2)	Ru(1)−C(21)	2.056(3)	Ru(1)−Cl(1)	2.4569(6)
N(4)−O(1)	1.145(3)				
N(4)−Ru(1)−C21	88.10(10)		N(4)−Ru(1)−N(2)		96.47(9)
C(21)−Ru(1)−N(2)	97.61(9)		N(4)−Ru(1)−N(3)		92.71(9)
C(21)−Ru(1)−N(3)	79.99(9)		N(2)−Ru(1)−N(3)		170.43(8)
N(4)−Ru(1)−N(1)	168.08(9)		C(21)−Ru(1)−N(1)		82.09(9)
N(2)−Ru(1)−N(1)	78.25(8)		N(3)−Ru(1)−N(1)		92.23(8)
N(4)−Ru(1)−Cl(1)	104.29(7)		C(21)−Ru(1)−Cl(1)		166.61(8)
N(2)−Ru(1)−Cl(1)	86.18(6)		N(3)−Ru(1)−Cl(1)		94.15(6)
N(1)−Ru(1)−Cl(1)	86.16(6)		O(1)−N(4)−Ru(1)		171.6(2)